Optical bistability in quantum dot with four cascade energy levels

C. YU*, L. SUN, H. ZHANG, F. CHEN
School of Physics and Optoelectronic Engineering, Yangtze University, Jingzhou, 434023, China
Institute of Quantum Optics and Information Photonics, Yangtze University, Jingzhou 434023, China

The optical bistability (OB) in a quantum dot (QD) system with four cascade energy levels by two coupling field inside unidirectional ring cavity is theoretically investigated. It is shown that the OB behavior can be controlled by suitable adjusting the system parameters such as the electronic cooperation parameter, the probe laser frequency detuning, the two coupling laser field and frequency detuning, and the decay rate. Such a system may be used in optical switching and other quantum information science.

(Received September 18, 2018; accepted April 8, 2019)

Keywords: Optical bistability, Quantum dot, Cascade, Optical switching

1. Introduction

OB, known as a system that has two stable output intensities for a single input one, has been widely investigated in both experiments and theories in the past decades. OB is studied in atoms confined in an optical ring cavity based on atomic coherence and interference effects, which can be controlled by phase fluctuation, electromagnetically induced transparency, spontaneously generated coherence, and so on [1-18].

Moreover, there has been an intense interest in the OB in the semiconductor quantum wells and dots because of its inherent advantages such as large electric dipole moments, the great flexibilities in devices, and so on. One recent study is OB in a symmetric quantum well-controled by choosing appropriate values of the electron sheet density and the intensity of the optical radiation [19]. Raheli [20] reported a novel phase sensitive quantum well nanostructure scheme to control OB by the relative phase of the applied fields. Tian et al. [21] reported OB can be controlled via tunneling induced quantum interference in triangular QD molecules. Taherzadeh et al. [22] proposed a scheme using a dielectric slab via inter-dot tunneling to achieve low threshold OB by at least one order of magnitude in respect to free QD molecules. In addition, the other OB programs in quantum wells and dots are also put forward recently [23-34].

In this work, we investigate the OB in a QD system with four cascade energy levels driven by two external electrical fields inside an optical ring cavity. The OB behavior can be easily controlled by two extra coupling laser fields via adjusting properly the corresponding system parameters.

2. Model and theory

Fig. 1 (a) shows a QD system with four cascade energy levels which is considered in this paper which also can be seen in [35].

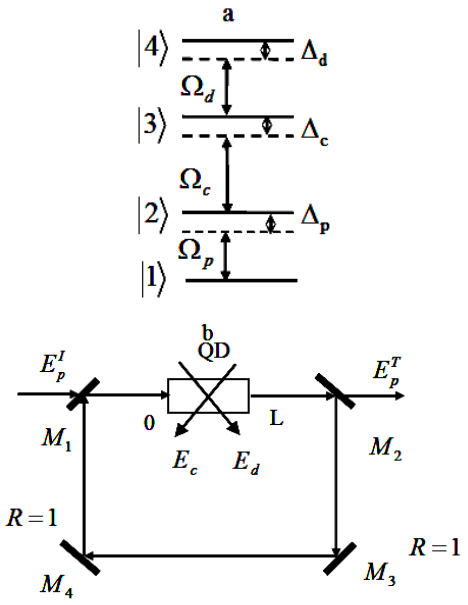

Fig. 1. The system energy levels and unidirectional ring cavity. (a) QD with four energy levels in cascade configuration interacting with two coupling fields and a probe optical field. (b) A unidirectional ring cavity with L-length QD sample and four mirrors. E_p^I *(*E_p^T*) is the incident (transmitted) field. For mirrors* M_1 *and* M_2*,* $R+T=1$ *and* R *(*T*) is the reflection (transmission) coefficient.* R *of mirrors* M_3 *and* M_4 *is 1*

Such a QD can be produced by self-assembled dot growth technology and optical properties can be modified by the impurities. $|1\rangle$ is the ground state without excitation. $|2\rangle$, $|3\rangle$ and $|4\rangle$ are the excited states of the QD. A probe laser field (with frequency ω_p and Rabi frequency Ω_{p}) couples the state $|1\rangle$ and $|2\rangle$. A coupling laser field (with frequency ω_c and Rabi frequency Ω_{c}) couples state $|2\rangle$ and $|3\rangle$. And another coupling laser field (with frequency ω_d and Rabi frequency Ω_{d}) couples state $|3\rangle$ and $|4\rangle$.

In the interaction picture, the system Hamiltonian can be written as ($\hbar = 1$),

$$H_{\mathrm{int}}^{I} = \begin{pmatrix} 0 & -\Omega_p & 0 & 0 \\ -\Omega_p & \Delta_p & -\Omega_c & 0 \\ 0 & -\Omega_c & \Delta_p + \Delta_c & -\Omega_d \\ 0 & 0 & -\Omega_d & \Delta_p + \Delta_c + \Delta_d \end{pmatrix} \quad (1)$$

where $\Omega_p = \mu_{12} E_p$ ($\Omega_{\mathrm{c}} = \mu_{23} E_{\mathrm{c}}, \Omega_{\mathrm{d}} = \mu_{34} E_{\mathrm{d}}$) is the Rabi frequency of the probe (two coupling) laser field, with μ_{ij} being the electric dipole moment of transition $|i\rangle$ and $|j\rangle$. $\Delta_p = \omega_{21} - \omega_p$ and $\Delta_c = \omega_{32} - \omega_c$ ($\Delta_d = \omega_{43} - \omega_d$) are the detuning of the probe and two coupling laser fields showing in Fig. 1(a). ω_{ij} is the transition frequency of the state $|i\rangle$ and $|j\rangle$.

At any time, the system quantum state $\Psi(t)$ obeys the Schrödinger equation as follows,

$$\frac{d}{dt}|\Psi(t)\rangle = -iH_{\mathrm{int}}^{I}(t)|\Psi(t)\rangle, \quad (2)$$

in which, $\Psi(t) = a_1|1\rangle + a_2|2\rangle + a_3|3\rangle + a_4|4\rangle$, where $a_j (j = 1-4)$ is the probability amplitude of the level $|j\rangle$. From Eq. (1) and (2), we can get

$$i\frac{d}{dt}a_1 = -\Omega_p a_2, \quad (3a)$$

$$i\frac{d}{dt}a_2 = (\Delta_p - i\gamma_2)a_2 - \Omega_p a_1 - \Omega_c a_3, \quad (3b)$$

$$i\frac{d}{dt}a_3 = (\Delta_p + \Delta_c - i\gamma_3)a_3 - \Omega_c a_2 - \Omega_d a_4, \quad (3c)$$

$$i\frac{d}{dt}a_4 = (\Delta_p + \Delta_c + \Delta_d - i\gamma_4)a_4 - \Omega_d a_3, \quad (3d)$$

$$|a_1|^2 + |a_2|^2 + |a_3|^2 + |a_4|^2 = 1, \quad (3e)$$

where $\gamma_i (i = 2\text{-}4)$, describing the corresponding total decay rate of the energy level $|i\rangle$, are added phenomenologically in the above equations.

In the steady state, solve Eq. (3) [30], we can get

$$\rho_{21} = a_2 a_1^* = \frac{\Omega_p B}{A} \cdot \frac{|A|^2}{|A|^2 + |\Omega_p B|^2 + |\Gamma_4 \Omega_c \Omega_p|^2 + |\Omega_d \Omega_c \Omega_p|^2}, \quad (4)$$

where, $\Gamma_2 = \Delta_p - i\gamma_2$, $\Gamma_3 = \Delta_p + \Delta_c - i\gamma_3$, $\Gamma_4 = \Delta_p + \Delta_c + \Delta_d - i\gamma_4$, $B = \Gamma_3\Gamma_4 - \Omega_d^2$, $A = \Gamma_2 B - \Gamma_4 \Omega_c^2$.

Now, the OB behavior of the above-described four-energy-level QD system will be studied in a unidirectional cavity (see Fig. 1 (b)). Under the slowly envelope approximation, the dynamics of the probe field in the optical cavity is governed by the Maxwell's equation. In the steady state and considering the boundary conditions, we can finally get [30],

$$\frac{\partial E_p}{\partial z} = iN\frac{\omega_p \mu_{21}}{2c\varepsilon_0}\rho_{21}, \quad (5a)$$

$$E_p(0) = \sqrt{T}E_p^I + RE_p(L), \quad (5b)$$

$$E_p(L) = E_p^T/\sqrt{T}, \quad (5c)$$

where c is the light speed in the vacuum. $N = \Gamma/V$ is the electronic number density. Γ is the optical confinement factor and V is the QD volume. $RE_p(L)$ in Eq. 5(b) shows the feedback mechanism of the mirrors.

In the mean-field limit, the input-output relationship

can be obtained from Eq. (5),

$$y = x - iC\rho_{21}, \tag{6}$$

where $C = N\omega_p L|\mu_{21}|^2/(2\hbar c\varepsilon_0 T)$ is the system electronic cooperation parameter, $x = \mu_{21}E_P^T/\hbar\sqrt{T}$ and $y = \mu_{21}E_P^I/\hbar\sqrt{T}$.

In addition, we also can discuss the linear and third-order susceptibility of our system. The probe susceptibility can be achieved from the Eq. (4) [19，36，37].

$$\chi_p = \frac{N|\mu_{21}|^2}{\hbar\varepsilon_0}\chi \tag{7}$$

$$\chi = \frac{\rho_{21}}{\Omega_p} \tag{8}$$

And χ can be expanded into the second order of the probe laser field Ω_p with neglecting the higher order smaller terms.

$$\chi = \chi^{(1)} + \chi^{(3)}\Omega_p^2 \tag{9}$$

where $\chi^{(1)}$ ($\chi^{(3)}$)is the first-order-linear (third-order-nonlinear) part of the susceptibility. So, we can get,

$$\chi^{(1)} = \frac{B}{A} \tag{10}$$

$$\chi^{(3)} = -\frac{B}{A}\bullet\frac{|B|^2 + |\Omega_c\Gamma_4|^2 + |\Omega_c\Omega_d|^2}{|A|^2} \tag{11}$$

3. Numerical results and discussions

In this article, the model works in the low temperature. For simplicity, we adopt $\gamma_2 = \gamma_3 = \gamma_4$ and all the parameters are scaled by the decay rate $\gamma_2 = 1meV$ in the first which can be influenced by the temperature and QD radius [38, 39].

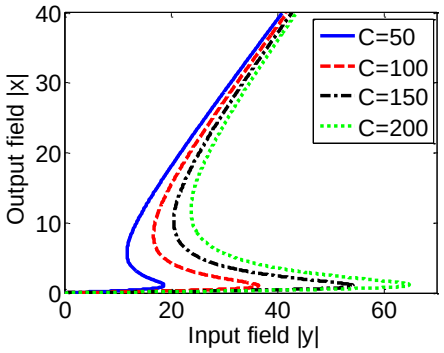

Fig.2. The effect of electronic cooperation parameter C *on the OB behavior. The other parameters are* $\Delta_p = \Delta_c = \Delta_d = 0, \Omega_c = \Omega_d = 10$

Firstly, in Fig. 2, the effect of the electronic cooperation parameter C on the OB is studied. We can find the increasing of the electronic cooperation parameter C greatly influences the threshold and the hysteresis cycle. It can be explained from $C = N\omega_p L|\mu_{21}|^2/(2\hbar c\varepsilon_0 T)$ where C is directly proportional to the electronic number density N . So, increasing N will enhance the sample absorption, which accounts for the raise of the OB threshold.

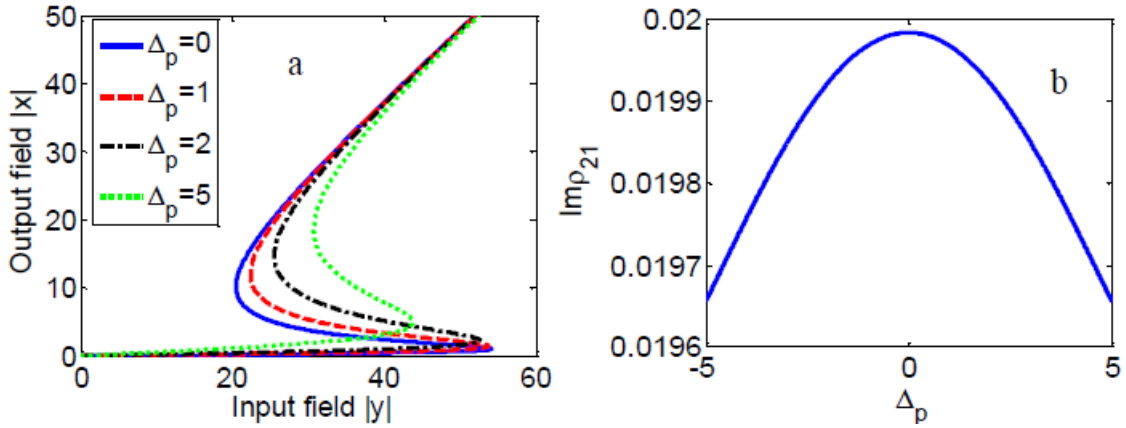

Fig. 3. The OB behavior and $\mathrm{Im}\rho_{21}$ *for different probing laser frequency detuning* Δ_p *. (a) The effect of the probing laser frequency detuning* Δ_p *on the OB behavior. (b)* $\mathrm{Im}\rho_{21}$ *as a function of* Δ_p *for* $\Omega_p = 50$*. The other parameters are* $C = 150, \Omega_c = \Omega_d = 10, \Delta_p = \Delta_c = \Delta_d = 0$

Secondly, in Fig. 3 (a), the effect of the probing laser frequency detuning Δ_p on the OB behavior is studied. It is found that the bistable threshold goes down with the increasing of the probing laser frequency detuning Δ_p. In order to have a better understanding about how the bistable threshold varies with the probing laser frequency detuning. We also plot the imaginary part of ρ_{21} ($\mathrm{Im}\rho_{21}$) in Fig. 3 (b). It is illustrated that $\mathrm{Im}\rho_{21}$ decreases with the increasing of the probe frequency detuning Δ_p, which accounts for the reduction of the absorption and the bistable threshold.

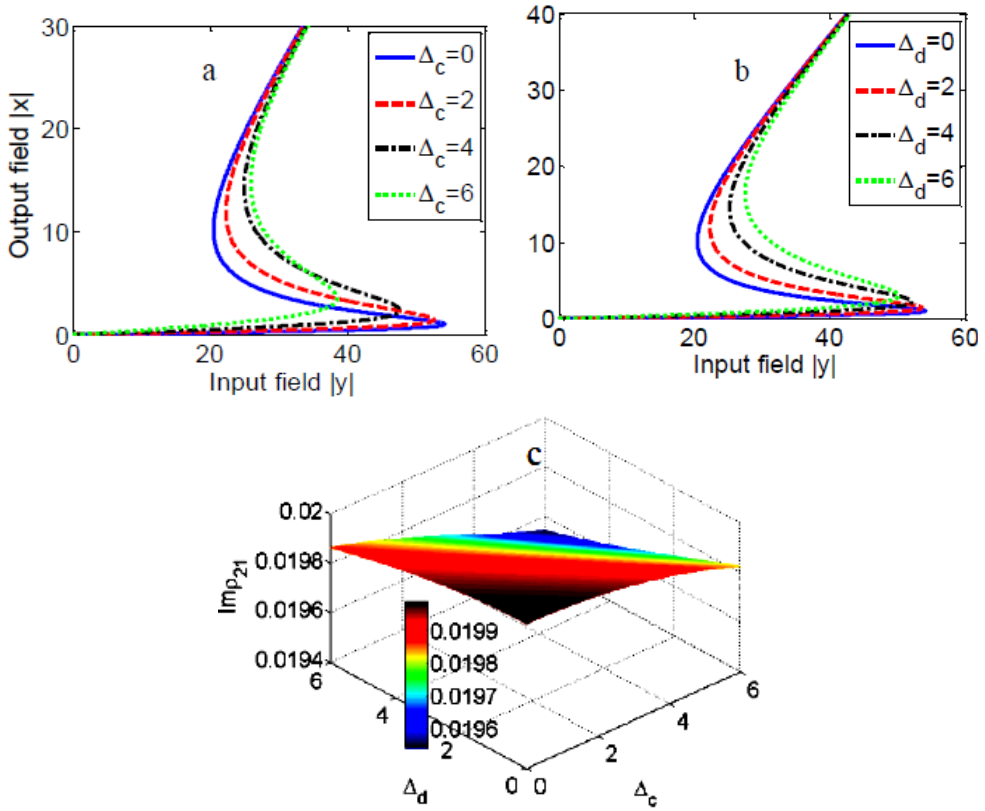

Fig. 4. The OB behavior and $\mathrm{Im}\rho_{21}$ *for different coupling laser frequency detuning* Δ_c *and* Δ_d *. (a) The effect of the coupling laser frequency detuning* Δ_c *on the OB behaviour.* $\Delta_d = 0$*. (b) The effect of the coupling laser frequency detuning* Δ_d *on the OB behaviour.* $\Delta_c = 0$*. (c)* $\mathrm{Im}\rho_{21}$ *as a function of* Δ_c *and* Δ_d*.* $\Omega_p = 50$*. The other parameters are,* $\Omega_c = \Omega_d = 10, \Delta_p = 0, C = 150$

Thirdly, we are interested in the effect of the coupling laser frequency detuning Δ_c and Δ_d on the OB behavior. So we plot the input-output field curves for different Δ_c in Fig. 4 (a) and Δ_d in Fig. 4 (b). In general, it is found that the OB threshold goes down with the increasing of the frequency detuning Δ_c and Δ_d. In order to have a better understanding about how the bistable threshold varies with the coupling laser frequency detuning. We also plot the imaginary part of ρ_{21} ($\mathrm{Im}\,\rho_{21}$) in Fig. 4 (c) for different Δ_c and Δ_d. It is illustrated that $\mathrm{Im}\,\rho_{21}$ decreases with the increasing of the coupling frequency detuning Δ_c and Δ_d, which accounts for the reduction of the absorption and the bistable threshold in Fig. 4 (a) and (b).

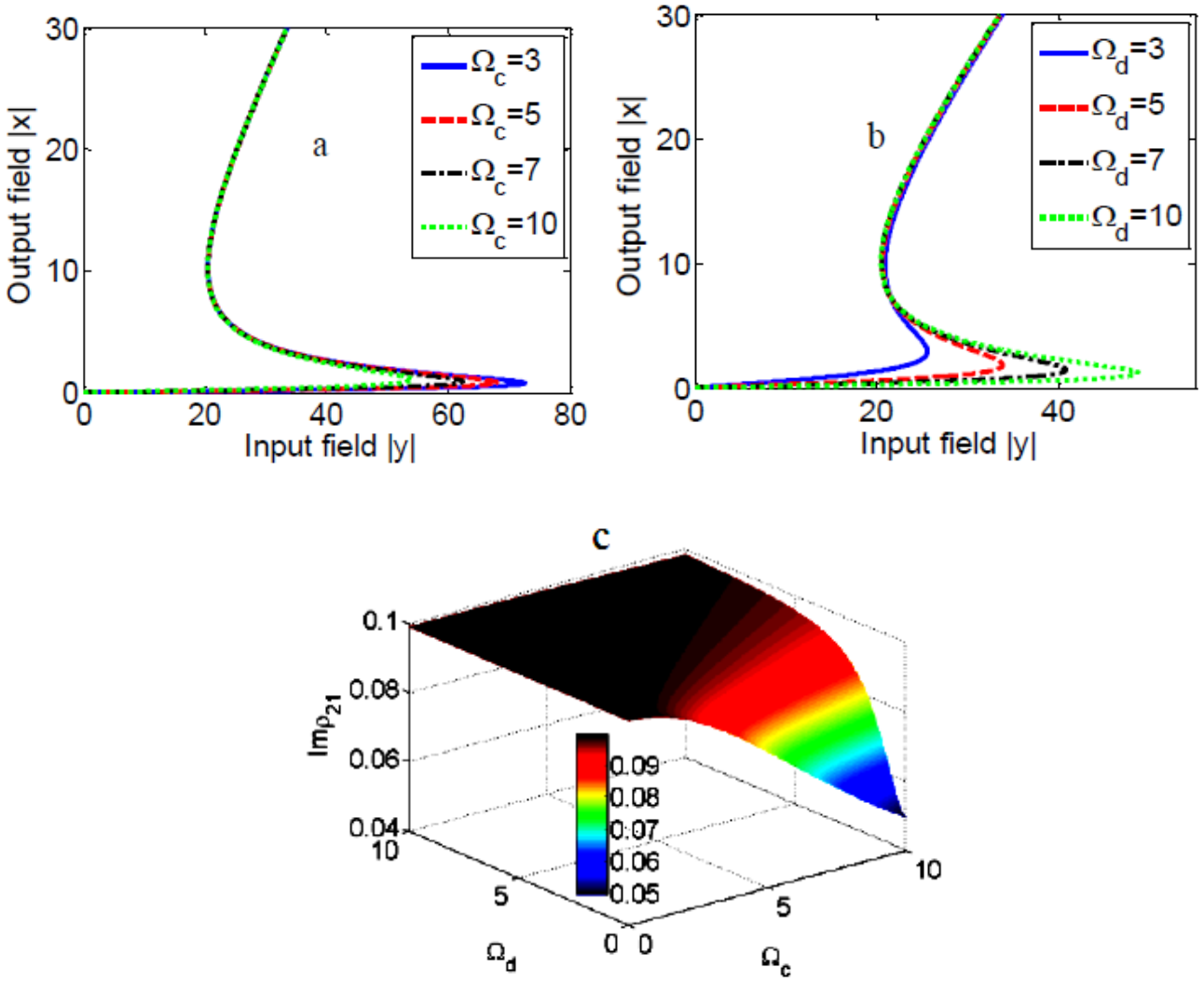

Fig. 5. The OB behavior and $\mathrm{Im}\,\rho_{21}$ *for different coupling laser field* Ω_c *and* Ω_d. *(a) The effect of the coupling laser field* Ω_c *on the OB behavior.* $\Omega_d = 10$. *(b) The effect of the coupling laser field* Ω_d *on the OB behavior.* $\Omega_c = 10$. *(c)* $\mathrm{Im}\,\rho_{21}$ *as a function of* Ω_c *and* Ω_d. $\Omega_p = 10$. *The other parameters are,* $\Delta_p = \Delta_c = \Delta_d = 0, C = 150$

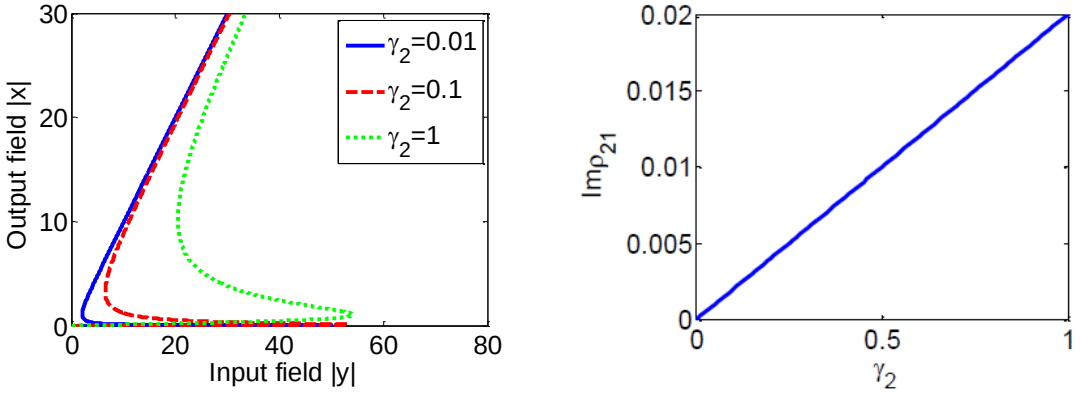

(a) *(b)*

Fig. 6. The OB behavior and $\mathrm{Im}\rho_{21}$ *for different decay rate* γ_2*. (a) The effect of the decay rate* γ_2 *on the OB behavior. The insert shows the hysteresis cycle near the threshold. (b)* $\mathrm{Im}\rho_{21}$ *as a function of* γ_2*. The other parameters are,* $\Delta_p = \Delta_c = \Delta_d = 0$, $\Omega_c = \Omega_d = 10$, $\Omega_p = 50$, $C = 150$

Fourthly, the effect of the coupling laser field Ω_c and Ω_d on the OB behavior can also be studied. We plot the input-output field curves for different Ω_c in Fig. 5 (a) and Ω_d in Fig. 5 (b). Clearly, the input-output field curves show converse behavior. The OB threshold goes down with the increasing of the coupling laser field Ω_c, and otherwise goes up with the increasing of the coupling laser field Ω_d. The main reason for the above phenomenon is that in Fig. 5 (c). It is illustrated that $\mathrm{Im}\rho_{21}$ decreases with the increasing of the coupling laser field Ω_c, and increases with the increasing of the coupling laser field Ω_d, which accounts for the changing of the bistable threshold in Fig. 4 (a) and (b).

Finally, we display the effect of the decay rate γ_2 on the OB behavior in Fig. 6 (a). We can find that the OB threshold goes up with the increasing of the decay rate γ_2, which can be interpreted in Fig. 6 (b). $\mathrm{Im}\rho_{21}$ increases with the increasing of the decay rate γ_2 which accounts for the changing of the OB threshold.

Before ending this part, let us pay attention to the cause of the OB in our system. By applying a strong coupling fields between $|2\rangle$ and $|3\rangle$ ($|3\rangle$ and $|4\rangle$), the system absorption and dispersion for the probe field between $|1\rangle$ and $|2\rangle$ are modified, and also the Kerr nonlinearity of the electronic medium is controlled, which make the hysteresis cycle and threshold alter consequently. The large OB threshold is due to the existence of a large absorption in the QD system, which causes the probe field hard to reach saturation. So, the OB curve can be adjusted by controlling the probe absorption with the methods discussed before. What is more, we also can theoretically study the linear and third nonlinear from Eq. (10) and (11) in our theory to explain the OB curve in detail. In our paper, we focus on the density matrix element ρ_{21} which contains the system total absorption enough to interpret the OB threshold variation trend in our knowledge.

4. Conclusion

In summary, using a QD system with four energy levels in cascade configuration interacting with two coupling fields and a probe optical field inside unidirectional ring cavity, we study the controllable OB behavior. Our results show that by suitable adjusting the system parameters such as the electronic cooperation parameter, the probe laser frequency detuning, the two coupling laser field and frequency detuning and the decay rate, we can efficiently control the OB behavior. As a result, the present research may be used in optical switching and other quantum information science.

Acknowledgements

This work is supported by the National Natural Science Foundation of China (Grant No. 11447182 and 11547007), the Yangtze Fund for Youth Teams of Science and Technology Innovation (Grant No. 2015cqt03).

References

[1] D. F. Walls, P. Zoller, Optics Communications **34**(2), 260 (1980).
[2] W. Harshawardhan, G. S. Agarwal, Physical Review A **53**(3), 1812 (1996).
[3] A. Joshi, M. Xiao, Physical Review Letters **91**(14), 143904 (2003).
[4] A. Joshi, A. Brown, H. Wang, M. Xiao, Physical Review A **67**(4), 041801 (2003)
[5] A. Joshi, W. Yang, M. Xiao, Physical Review A **68**(1), 015806 (2003).
[6] A. Joshi, W. Yang, M. Xiao, Physics Letters A **315**(3), 203 (2003).
[7] N. M. Litchinitser, I. R. Gabitov, A. I. Maimistov,

Physical Review Letters **99**(11), 113902 (2007).
[8] J. H. Li, X. Y. Lü, J. M. Luo, Q. J. Huang, Physical Review A **74**(3), 035801 (2006).
[9] Z. Wang, M. Xu, Optics Communications **282**(8), 1574 (2009).
[10] Z. H. Xiao, K. Kim, Optics Communications **283**(10), 2178 (2010).
[11] S. H. Asadpour, A. Eslami-Majd, Journal of Luminescence **132**(6), 1477 (2012).
[12] Z. Wang, A. X. Chen, Y. Bai, R. K. Lee, J. Opt. Soc. Am. B **29**(10), 2891 (2012).
[13] S. H. Asadpour, M. Jaberi, H. R. Soleimani, J. Opt. Soc. Am. B **30**(7), 1815 (2013).
[14] A. Jafari, R. Naderali, S. Bakkeshizadeh, Optical and Quantum Electronics **48**(1), 55 (2016).
[15] H. R. Hamedi, Laser Physics **27**(6), 066002 (2017).
[16] A. A. Nejad, H. R. Askari, H. R. Baghshahi, Applied Optics **56**(10), 2816 (2017).
[17] I. Karabulut, Superlattices and Microstructures **111**, 181 (2017).
[18] A. Raheli, Brazilian Journal of Physics **48**(2), 111 (2018).
[19] S. H. Asadpour, H. R. Hamedi, H. R. Soleimani, Journal of Modern Optics **60**(8), 659 (2013).
[20] M. Sahrai, S. H. Asadpour, R. Sadighi-Bonabi, Journal of Luminescence **131**(11), 2395 (2011).
[21] S. C. Tian, R. G. Wan, C. Z. Tong, J. L. Zhang, X. N. Shan, X. H. Fu, Y. G. Zeng, L. Qin, Y. Q. Ning, AIP Advances **5**(6), 067144 (2015).
[22] S. Taherzadeh, R. Nasehi, M. Mahmoudi, Laser Physics **25**(4), 045901 (2015).
[23] J. Li, X. Hao, J. Liu, X. Yang, Physics Letters A **372**(5), 716 (2008).
[24] M. A. Antón, F. Carreño, O. G. Calderón, S. Melle, Optics Communications **281**(12), 3301 (2008).
[25] J. Li, R. Yu, J. Liu, P. Huang, X. Yang, Physica E **41**(1), 70 (2008).
[26] Z. Wang, H. Fan, Journal of Luminescence **130**(11), 2084 (2010).
[27] Z. Wang, B. Yu, JOSA B **30**(11), 2915 (2013).
[28] Z. Wang, S. Zhen, X. Wu, J. Zhu, Z. Cao, B. Yu, Optics Communications **304**, 7 (2013).
[29] A. Vafafard, S. Goharshenasan, N. Nozari, A. Mortezapour, M. Mahmoudi, Journal of Luminescence **134**, 900 (2013).
[30] S. C. Tian, R. G. Wan, C. Z. Tong, Y. Q. Ning, J. Opt. Soc. Am. B **31**(11), 2681 (2014).
[31] S. H. Asadpour, H. R. Soleimani, Optics Communications **315**, 347 (2014).
[32] H. R. Hamedi, Physica B **449**, 5 (2014).
[33] S. H. Asadpour, H. R. Soleimani, Physica B: Condensed Matter **440**, 124 (2014)
[34] C. Yu, L. Sun, H. Zhang, F. Chen, IET Optoelectronics **12**(4), 215 (2018).
[35] V. Pavlović, Optik **127**(16), 6351 (2016).
[36] S. H. Asadpour, H. R. Hamedi, Optical and Quantum Electronics **45**(1), 11 (2013).
[37] S. H. Asadpour, Applied Optics **56**(8), 2201 (2017).
[38] G. Rezaei, S. S. Kish, Superlattices and Microstructures **53**, 99 (2013).
[39] B. Krause, T. H. Metzger, Physical Review B **72**(8), 085339 (2005).

*Corresponding author: chchyu@yangtzeu.edu.cn